

3D printed vascularized device for subcutaneous transplantation of human islets

*Original*

3D printed vascularized device for subcutaneous transplantation of human islets / Farina, Marco; Ballerini, Andrea; Fraga, Daniel; Nicolov, Eugenia; Hogan, Matthew; Demarchi, Danilo; Scaglione, Francesco; Sabek, Omaira; Horner, Philip; Thekkedath, Usha; Gaber, Osama; Grattoni, Alessandro. - In: BIOTECHNOLOGY JOURNAL. - ISSN 1860-6768. - 12:9(2017).

*Availability:*

This version is available at: 11583/2674122 since: 2020-09-06T16:22:58Z

*Publisher:*

WILEY-VCH

*Published*

DOI:

*Terms of use:*

This article is made available under terms and conditions as specified in the corresponding bibliographic description in the repository

*Publisher copyright*

Wiley preprint/submitted version

(Article begins on next page)



### 3D printed vascularized device for subcutaneous transplantation of human islets

Journal:	<i>Biotechnology Journal</i>
Manuscript ID	biot.201700169.R1
Wiley - Manuscript type:	Research Article
Date Submitted by the Author:	n/a
Complete List of Authors:	Farina, Marco; Houston Methodist Research Institute, Nanomedicine; Politecnico di Torino, Electronics and Telecommunications Ballerini, Andrea; Houston Methodist Hospital; Universita degli Studi di Milano, Department of Oncology and Onco-Hematology Fraga, Daniel; Houston Methodist Hospital, Surgery Nicolov, Eugenia; Houston Methodist Research Institute, Nanomedicine Hogan, Matthew; Houston Methodist Research Institute, Center of Neuroregeneration Demarchi, Danilo; Politecnico di Torino, Electronics and Telecommunications Scaglione, Francesco; Universita degli Studi di Milano, Department of Oncology and Onco-Hematology Sabek, Omaima; Houston Methodist Hospital, Surgery Horner, Philip; Houston Methodist Research Institute, Center of Neuroregeneration Thekkedath, Usha; Houston Methodist Research Institute, Nanomedicine Gaber, Osama; Houston Methodist Hospital, Surgery Grattoni, Alessandro; Houston Methodist Research Institute, Nanomedicine
Primary Keywords:	Biomaterials, Medical biotechnology
Secondary Keywords:	Bioencapsulation, Cellular therapy, Medical applications
Additional Keywords:	

1  
2  
3 Rapid Communication

4  
5 **3D printed vascularized device for subcutaneous transplantation of human islets**

6  
7  
8  
9 **Authors:** Marco Farina<sup>\*1,4</sup>, Andrea Ballerini<sup>\*1,5</sup>, Daniel Fraga<sup>2</sup>, Eugenia Nicolov, Matthew Hogan<sup>3</sup>, Danilo  
10 Demarchi<sup>4</sup>, Francesco Scaglione<sup>5</sup>, Oaima Sabek<sup>2</sup>, Philip Horner<sup>3</sup>, Usha Thekkedath<sup>1</sup>, Osama Gaber<sup>\*\*2</sup>,  
11 Alessandro Grattoni<sup>\*\*1</sup>

12  
13  
14  
15 <sup>1</sup>Department of Nanomedicine, Houston Methodist Research Institute, Houston, TX; <sup>2</sup>Department of  
16 Surgery, Houston Methodist Hospital, Houston, TX; <sup>3</sup>Center for Neuroregeneration, Houston  
17 Methodist Research Institute, Houston, TX; <sup>4</sup>Department of Electronics and Telecommunications,  
18 Politecnico di Torino, Torino, Italy; <sup>5</sup>Department of Oncology and Onco-Hematology, University of  
19 Milan, Milan, Italy

20  
21  
22  
23  
24  
25  
26  
27  
28  
29  
30  
31  
32  
33  
34  
35  
36  
37  
38  
39  
40  
41  
42  
43  
44  
45  
46  
47  
48  
49  
50  
51  
52  
53  
54  
55  
56  
57  
58  
59  
60  

\*Co-first; \*\* Co-senior.

30  
31  
32  
33  
34  
35  
36  
37  
38  
39  
40  
41  
42  
43  
44  
45  
46  
47  
48  
49  
50  
51  
52  
53  
54  
55  
56  
57  
58  
59  
60  

**Correspondence:** Dr. Alessandro Grattoni, Chair, Department of Nanomedicine, Houston Methodist  
Research Institute, 6670 Bertner Avenue, R8-216, Houston, TX, 77030

**E-mail:** agrattoni@houstonmethodist.org

**Keywords:** 3D printing, Diabetes, Encapsulations, Islets, Transplantations

**Abbreviations:** FDM, Fused Deposition Method; H&E, hematoxylin and eosin; IEQ, Islet equivalent;  
PLM, platelet lysate matrix; PLA, polylactic acid; SEM, scanning electron microscopy; VEGF, vascular  
endothelial growth factor.

**Abstract**

Transplantation of pancreatic islets or stem cell derived insulin secreting cells is an attractive treatment strategy for diabetes. However, islet transplantation is associated with several challenges including function-loss associated with dispersion and limited vascularization as well as the need for continuous immunosuppression. To overcome these limitations, here we present a novel 3D printed and functionalized encapsulation system for subcutaneous engraftment of islets or islet like cells. The devices were 3D printed with polylactic acid and the surfaces treated and patterned to increase the hydrophilicity, cell attachment and proliferation. Surface treated encapsulation systems were implanted with growth factor enriched platelet gel, which helped to create a vascularized environment before loading human islets. The device protected the encapsulated islets from acute hypoxia and kept them functional. The adaptability of the encapsulation system was demonstrated by refilling some of the experimental groups transcutaneously with additional islets.

## Introduction

Transplantation of pancreatic islets or stem cell derived insulin secreting cells is an attractive treatment strategy for diabetes<sup>1,2</sup>. However, islet transplantation is associated with several challenges including function-loss associated with dispersion and limited vascularization as well as the continuous need for immunosuppression<sup>3</sup>. In spite of early success with intrahepatic transplantation, widespread use of islet transplantation has been hampered by poor long-term survival of the graft<sup>3,4</sup>. After intra-hepatic or intravascular islet transplantation, graft function is lost rapidly due to dispersion of transplanted tissue, damage to graft caused by blood-mediated inflammatory reaction, and the hypoxic stress due to the limited ingrowth of new blood vessels<sup>5</sup>. High oxygen demand and the need for physiological architecture necessitate a highly vascularized and three-dimensional system for the long-term survival and function of transplanted islets. In addition, a minimally invasive and accessible site is fundamental for implantation, replenishment and graft retrieval. Retrievability is important when using engineered stem cells, whose long term fate and potential for tumor formation are not well known.<sup>6</sup> The subcutaneous space could serve as an ideal implantation site, if we can overcome challenges of low oxygen tension and poor vascularity and offer mechanical protection to transplanted cells<sup>7,8</sup>. To meet these needs, we designed an adaptable, scalable and refillable encapsulation system for subcutaneous transplantation of cells. In this work, we demonstrate the feasibility to 3D print an innovative encapsulation system and evaluate its vascularization after subcutaneous implantation. The system was loaded transcutaneously with human pancreatic islets and their long-term survival and function were studied in an immunocompromised mouse model.

## Materials & Methods

Discoidal encapsulation devices (8 mm in diameter and 2.5 mm in thickness, Fig. 1a) suitable for holding up to 5,000 islets were printed adopting a Fused Deposition Method (FDM) based 3D printer (Replicator™ 2X, MakerBot Industries) and medical grade polylactic acid (PLA, Foster Corporation). The two inner surfaces were composed of an array of micro-reservoirs (300 μm x 300 μm) to house the transplanted islets individually, maintaining them in close proximity while avoiding clustering. These micro-reservoirs are connected to surrounding tissues by an array of square

1  
2  
3 microchannels (100  $\mu\text{m}$  x 100  $\mu\text{m}$  cross section, 50  $\mu\text{m}$  length) to allow for the growth of  
4  
5 transmembrane blood vessels in view of graft vascularization. The devices featured a loading port (1  
6  
7 mm diameter) for transcutaneous cell loading. Device surfaces were treated with Argon and Oxygen  
8  
9 plasma (March plasma etcher, Nordson). The power (30W) and gas flow (150mTorr) were kept  
10  
11 constant, while changing the exposure time (30, 90, 120 and 150 seconds). The nanopatterning of the  
12  
13 device surfaces was evaluated before and after treatment by scanning electron microscopy (SEM)  
14  
15 (Nova NanoSEM, FEI) for channel quality and size (Fig. 1b-c). Hydrophilicity was evaluated by  
16  
17 measuring the water contact angle and surface roughness was evaluated by atomic-force microscopy  
18  
19 set in tapping mode (BioScope Catalyst, Bruker Instruments, Texas).<sup>9</sup>

20  
21 The encapsulation systems were evaluated in nude mice (Nu/Nu, female, 8-10 week old), after  
22  
23 receiving approval by the Institutional Animal Care and Use Committee of Houston Methodist  
24  
25 Research Institute. Surface treated and sterilized devices, loaded with platelet-lysate matrix (PLM)  
26  
27 enriched with VEGF at two different concentrations (0.5 and 5  $\mu\text{g}/\text{ml}$ ), were implanted subcutaneously  
28  
29 in the mice dorsum (n=12 per group). At 1, 2, and 4 weeks post implantation, 4 mice per group were  
30  
31 euthanized and the graft explanted for the histological assessment of vascularization and innervation.  
32  
33 The implant and surrounding tissues were harvested, and processed for histopathology evaluation of  
34  
35 tissue response to the implanted device. CD31 antibody (Abcam, ab28364) and a pan-axonal antibody  
36  
37 (Cambridge Bioscience, SMI-312R-100) were used to assess vascularization and innervation,  
38  
39 respectively. A second experiment was performed in nude mice (n=5 per group) to evaluate insulin  
40  
41 release from human islets transplanted into a prevascularized device. Human pancreatic islets (2,000  
42  
43 IEQ per mice) were injected with a 22 G needle transcutaneously into the encapsulation system 4  
44  
45 weeks after device implantation. Islets implanted under the kidney capsule served as positive  
46  
47 control.<sup>10</sup> Human insulin (ultra-sensitive human insulin ELISA kit, Alpco) and blood glucose  
48  
49 (OneTouch® Glucometer, Johnson and Johnson) levels were assessed weekly and body weight was  
50  
51 monitored throughout the experiment. Intra peritoneal glucose tolerance test (IPGTT) was performed  
52  
53 weekly to assess insulin secretion, in response to stimuli, from the transplanted islets. A subsequent  
54  
55 test was performed on the same animal cohort to demonstrate the refillability of the implant. Twelve  
56  
57  
58  
59  
60

1  
2  
3 weeks after the first injection, additional human islets (2,000 IEQ per mice) were injected  
4  
5  
6  
7  
8  
9  
10  
11  
12  
13  
14  
15  
16  
17  
18  
19  
20  
21  
22  
23  
24  
25  
26  
27  
28  
29  
30  
31  
32  
33  
34  
35  
36  
37  
38  
39  
40  
41  
42  
43  
44  
45  
46  
47  
48  
49  
50  
51  
52  
53  
54  
55  
56  
57  
58  
59  
60

trancutaneously in all groups where the insulin production was lower than 0.125  $\mu$ IU/ml.

All data are represented as average and standard error of the mean (SEM) and statistical analysis performed using Student's paired t-test. A value of  $p < 0.05$  was considered statistically significant. GraphPad Software, Inc. was used for the analysis.

## Results & Discussion

Transplantation of islets on porous biomaterials has emerged as a promising strategy for long-term islet function facilitating rapid tissue ingrowth, vascularization and innervation providing oxygen, nutrition, and waste removal<sup>11</sup>. Recognizing such needs for an islet and cell encapsulation system, we are working on new strategies to deliver cells subcutaneously<sup>9,12</sup>. The architecture of the proposed device is designed to maintain pancreatic islets close to blood vessels in a growth factor enriched environment, but separated from each other to mimic the physiological architecture in the pancreas and avoid cell crowding.

To increase the biointegration of the encapsulation system, we decided to use PLA, which is a widely adopted polymer in biomedical devices, biocompatible, and presents good elasticity and mechanical strength suitable for subcutaneous implantation<sup>13-15</sup>. Due to the chiral nature of lactic acid, PLA is hydrophobic with low cell adhesion properties. Surface treatment with plasma improves the low surface free energy of different materials and offers a solvent-free technique capable of changing the wettability, surface roughness and surface chemistry of polymers, enhancing cell proliferation and viability<sup>16-18</sup>. Plasma activation also increases PLA's surface free energy forming a broad variety of functional groups on the surface, including polar groups, which drastically change wettability and have a positive effect on material-cell interactions. Previous work from our group demonstrated that plasma treatment substantially increased the hydrophilicity of the surface and reduced the contact angle, which remained stable over 30 days in phosphate buffered saline (PBS)<sup>9</sup>. Here we looked at the effect of plasma exposure time on surface patterning and roughness and compared Oxygen and Argon treatments. As shown in Fig. 1d, both treatments increased surface roughness, reaching a maximum value, after which the roughness diminished with continued exposure, possibly due to eventual

1  
2  
3 etching of the crystalline regions. It was also noticed that the Oxygen treatment cause deeper patterns  
4  
5 (4.63 nm with Argon and 26.45 nm with Oxygen,  $p < 0.01$ , Fig. 1e), which has been demonstrated to be  
6  
7 beneficial for cell attachment and proliferation<sup>19</sup>.

8  
9 We then investigated the in vivo vascularization and innervation of Oxygen treated devices  
10  
11 after subcutaneous implantation in nude mice. We used nude mice as they show an inflammatory  
12  
13 response to a foreign body, but allow for transplantation with human islets without the need for  
14  
15 immunosuppression. It has been broadly demonstrated that vascularization of the graft is the key for  
16  
17 successful engraftment of islet transplants<sup>7,20</sup>. Prevascularization could mitigate the issue of acute  
18  
19 hypoxia which was shown to result in islet apoptosis and graft failure<sup>3</sup>. To stimulate  
20  
21 neovascularization and to support the islet viability and function for a period of time after  
22  
23 transplantation we used devices loaded with biological gels with different VEGF concentrations<sup>21-23</sup>.  
24  
25 An acute inflammatory response to the foreign body was present in the first week after device  
26  
27 implantation, mainly in the VEGF groups, and subsided with time, leaving a rim of vascularized  
28  
29 connective tissue around the device at week 4 (Fig. 2). Indeed, the neutrophils, which are considered  
30  
31 of impact for the development of the inflammatory response which leads to the formation of the  
32  
33 fibrotic capsule<sup>24</sup>, were almost absent from the second week (Fig. 2 a-i). The red arrows in Fig. 2  
34  
35 indicate the protrusion of the surrounding subcutaneous tissue into the devices. Tissue samples were  
36  
37 taken from the side of the device closer to the skin, representing the subcutaneous environment. We  
38  
39 noticed a positive trend between VEGF concentration and the number of vessels stained by CD31 (Fig.  
40  
41 2j-m). However, after 4 weeks, we noticed calcification in the VEGF 5  $\mu\text{g}/\text{ml}$  sample (Fig. 2i) as evident  
42  
43 by the dark spots in high density close to the tissue-implant interface. It was observed that in 4 weeks  
44  
45 the subcutaneous tissue and the inside of the device were vascularized (Fig. n-o). Based on these  
46  
47 results, 0.5  $\mu\text{g}/\text{ml}$  VEGF was selected for further studies. Finally, we also found nerve bundles in the  
48  
49 proximity of the device (Figure 2p-q), indicating their potential to reach the transplanted islets.  
50  
51 Further studies are necessary to prove and quantify islet innervation. After proving the device  
52  
53 vascularization, we performed a second experiment injecting human islet into a prevascularized  
54  
55 device. We observed detectable levels of human insulin from week 4, but at lower levels compared to  
56  
57 the positive control ( $p < 0.001$ ). As described in various islet encapsulation models, there is a lag time  
58  
59  
60

1  
2  
3 for adequate function until the transplanted islets are vascularized<sup>7,25</sup>. The prevascularization of the  
4 device appeared to have helped encapsulated islets to overcome the initial post implant injury, but it  
5 takes a few weeks for the transplanted cells to develop mature vasculature and be functional.  
6  
7

8  
9 A second load of islets (2,000 IEQ) into vascularized devices increased the insulin levels (~10  $\mu$ IU/ml)  
10 to values that were comparable to the kidney capsule transplantation ( $p>0.05$ ). Additionally, the  
11 devices were well tolerated and animals showed comparable basal glucose level and weight,  
12 demonstrating that the presence of additional islets is not associated with hypoglycemia.  
13  
14  
15  
16  
17

## 18 19 20 **Conclusion**

21 In this study, we showed that the subcutaneous implantation of a 3D printed and functionalized cell  
22 encapsulation system generates adequate and prompt vascularization of the graft. Vascularization was  
23 enhanced by the ability to dispense pro-angiogenic factors, such as VEGF, which is also known to  
24 increase islet viability and function<sup>22</sup>. In addition, the device could protect the graft, while the islets are  
25 being vascularized, from initial transplant site stressors and support their long-term survival. The  
26 transcutaneous refillability of the device offers opportunities for cell supplementation, without  
27 surgical retrieval and re-implantation, to accommodate changing physiological needs. This will be of  
28 significant advantage in the case of the growing children with diabetes. Moreover, the reservoir  
29 structure permits the potential retrievability of the graft, which is important for stem cell derived  
30 engineered cells, undergoing malignant or other unwanted transformations. Though the current  
31 studies were done in immunodeficient animal models, the device can be incorporated with local  
32 delivery of immunomodulators, which will expand its evaluation in immunocompetent diabetic  
33 animals<sup>26,27</sup>. Further studies in diabetic animal models are required to prove the efficacy of this  
34 versatile encapsulation system for diabetes cell therapy.  
35  
36  
37  
38  
39  
40  
41  
42  
43  
44  
45  
46  
47  
48  
49  
50

## 51 52 53 **Acknowledgements**

54 The authors express their sincere gratitude to the Vivian L. Smith Foundation for the support, and The  
55 Methodist Physician organization that made this investigation possible. Pancreata was provided by  
56 LifeGift Organ Procurement Organization, Houston Texas. Some research islets were provided by the  
57  
58  
59  
60

1  
2  
3 Integrated Islet Distribution Program (City of Hope, Duarte CA). We thank Dr. Jianhua (James) Gu from  
4 the electron microscopy core, Dr. Andreana L. Rivera and Dr. Yulan Ren from the research pathology  
5 core of the Houston Methodist Research Institute.  
6  
7  
8  
9

#### 10 **Conflict of interest**

11  
12 Authors declare that they have competing interests as the encapsulation system described in this  
13 paper is currently under invention disclosure.  
14  
15  
16  
17  
18  
19  
20  
21  
22  
23  
24  
25  
26  
27  
28  
29  
30  
31  
32  
33  
34  
35  
36  
37  
38  
39  
40  
41  
42  
43  
44  
45  
46  
47  
48  
49  
50  
51  
52  
53  
54  
55  
56  
57  
58  
59  
60

For Peer Review

## References

1. Ahearn, A. J., Parekh, J. R. & Posselt, A. M. Islet transplantation for Type 1 diabetes: where are we now? *Expert Rev. Clin. Immunol.* **11**, 59–68 (2015).
2. Zinger, A. & Leibowitz, G. Islet transplantation in type 1 diabetes: hype, hope and reality - a clinician's perspective. *Diabetes Metab. Res. Rev.* **30**, 83–87 (2014).
3. Brennan, D. C. *et al.* Long-Term Follow-Up of the Edmonton Protocol of Islet Transplantation in the United States. *Am. J. Transplant. Off. J. Am. Soc. Transplant. Am. Soc. Transpl. Surg.* (2015). doi:10.1111/ajt.13458
4. Shapiro, A. M. J. *et al.* International trial of the Edmonton protocol for islet transplantation. *N. Engl. J. Med.* **355**, 1318–30 (2006).
5. Lau, J. *et al.* Beneficial role of pancreatic microenvironment for angiogenesis in transplanted pancreatic islets. *Cell Transplant.* **18**, 23–30 (2009).
6. Pagliuca, F. W. & Melton, D. A. How to make a functional beta-cell. *Development* **140**, 2472–2483 (2013).
7. Pepper, A. R. *et al.* A prevascularized subcutaneous device-less site for islet and cellular transplantation. *Nat. Biotechnol.* **33**, 518–23 (2015).
8. Andrades, P. *et al.* Subcutaneous pancreatic islet transplantation using fibrin glue as a carrier. *Transplant. Proc.* **39**, 191–2 (2007).
9. Sabek, O. M. *et al.* Three-dimensional printed polymeric system to encapsulate human mesenchymal stem cells differentiated into islet-like insulin-producing aggregates for diabetes treatment. *J. Tissue Eng.* **7**, 2041731416638198 (2016).
10. Sabek, O. M., Fraga, D. W., Minoru, O., McClaren, J. L. & Gaber, A. O. Assessment of human islet viability using various mouse models. *Transplant. Proc.* **37**, 3415–6 (2005).
11. Scharp, D. W. & Marchetti, P. Encapsulated islets for diabetes therapy: History, current progress, and critical issues requiring solution. *Adv. Drug Deliv. Rev.* **67–68**, 35–73 (2014).
12. Sabek, O. M. *et al.* Characterization of a nanogland for the autotransplantation of human pancreatic islets. *Lab. Chip* **13**, 3675–88 (2013).

- 1  
2  
3 13. Onuki, Y., Bhardwaj, U., Papadimitrakopoulos, F. & Burgess, D. J. A review of the  
4 biocompatibility of implantable devices: current challenges to overcome foreign body response. *J.*  
5 *Diabetes Sci. Technol.* **2**, 1003–15 (2008).  
6  
7
- 8  
9 14. Lasprilla, A. J. R., Martinez, G. A. R., Lunelli, B. H., Jardini, A. L. & Filho, R. M. Poly-lactic acid  
10 synthesis for application in biomedical devices - a review. *Biotechnol. Adv.* **30**, 321–8 (2012).  
11
- 12 15. *Poly(Lactic Acid): Synthesis, Structures, Properties, Processing, and Applications.* (John Wiley &  
13 Sons, Inc., 2010).  
14  
15
- 16 16. Shah, A., Shah, S., Mani, G., Wenke, J. & Agrawal, M. Endothelial cell behaviour on gas-plasma-  
17 treated PLA surfaces: the roles of surface chemistry and roughness. *J. Tissue Eng. Regen. Med.* **5**,  
18 301–12 (2011).  
19  
20
- 21 17. Jacobs, T. *et al.* Plasma surface modification of polylactic acid to promote interaction with  
22 fibroblasts. *J. Mater. Sci. Mater. Med.* **24**, 469–478 (2012).  
23  
24
- 25 18. Morent, R., De Geyter, N., Desmet, T., Dubruel, P. & Leys, C. Plasma Surface Modification of  
26 Biodegradable Polymers: A Review. *Plasma Process. Polym.* **8**, 171–190 (2011).  
27  
28
- 29 19. Bacakova, L., Filova, E., Parizek, M., Ruml, T. & Svorcik, V. Modulation of cell adhesion,  
30 proliferation and differentiation on materials designed for body implants. *Biotechnol. Adv.* **29**, 739–  
31 767 (2011).  
32  
33
- 34 20. Pepper, A. R., Gala-Lopez, B., Ziff, O. & Shapiro, A. M. J. Revascularization of transplanted  
35 pancreatic islets and role of the transplantation site. *Clin. Dev. Immunol.* **2013**, 352315 (2013).  
36  
37
- 38 21. Jabs, N. *et al.* Reduced insulin secretion and content in VEGF-a deficient mouse pancreatic  
39 islets. *Exp. Clin. Endocrinol. Diabetes Off. J. Ger. Soc. Endocrinol. Ger. Diabetes Assoc.* **116 Suppl**, S46–  
40 9 (2008).  
41  
42
- 43 22. Lammert, E. *et al.* Role of VEGF-A in vascularization of pancreatic islets. *Curr. Biol. CB* **13**,  
44 1070–4 (2003).  
45  
46
- 47 23. Watada, H. Role of VEGF-A in pancreatic beta cells. *Endocr. J.* **57**, 185–191 (2010).  
48  
49
- 50 24. Anderson, J. M., Rodriguez, A. & Chang, D. T. Foreign body reaction to biomaterials. *Semin.*  
51 *Immunol.* **20**, 86–100 (2008).  
52  
53  
54  
55  
56  
57  
58  
59  
60

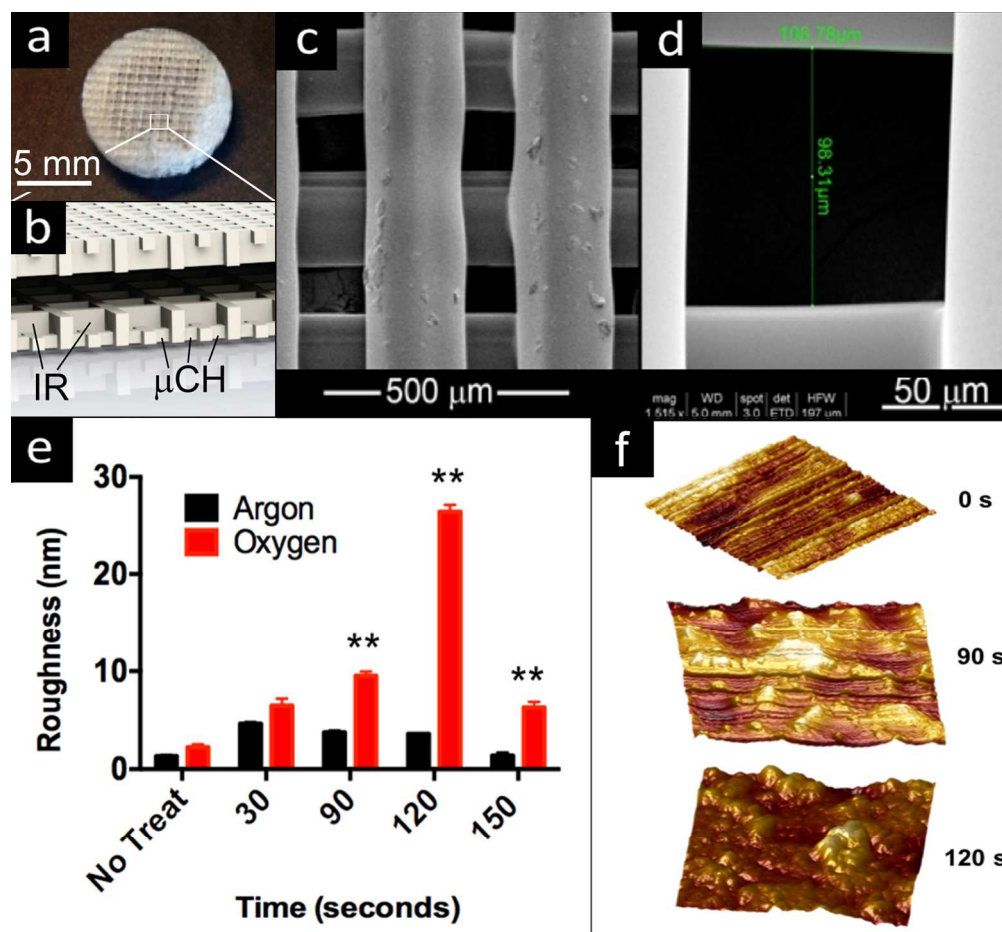
- 1  
2  
3 25. Szot, G. L. *et al.* Tolerance induction and reversal of diabetes in mice transplanted with human  
4 embryonic stem cell-derived pancreatic endoderm. *Cell Stem Cell* **16**, 148–157 (2015).  
5  
6  
7 26. Ferrati, S. *et al.* Leveraging nanochannels for universal, zero-order drug delivery in vivo. *J.*  
8  
9 *Control. Release Off. J. Control. Release Soc.* **172**, 1011–9 (2013).  
10  
11 27. Van Belle, T. & von Herrath, M. Immunosuppression in islet transplantation. *J. Clin. Invest.* **118**,  
12 1625–1628 (2008).  
13  
14  
15  
16  
17  
18  
19  
20  
21  
22  
23  
24  
25  
26  
27  
28  
29  
30  
31  
32  
33  
34  
35  
36  
37  
38  
39  
40  
41  
42  
43  
44  
45  
46  
47  
48  
49  
50  
51  
52  
53  
54  
55  
56  
57  
58  
59  
60

For Peer Review

1  
2  
3 **Figure 1.** Mouse prototype of the 3D-printed PLA encapsulation system (a) with magnification under  
4 SEM (b, c). PLA superficial roughness measurements after Argon and Oxygen plasma treatments,  
5 changing time of application (0, 30, 90, 120, and 150 seconds) (d). AFM pictures of PLA surface treated  
6 with Oxygen plasma after 0, 90 and 120 seconds (e). Average and Standard Error of the Mean are  
7 represented. \*\*  $p < 0.01$ .

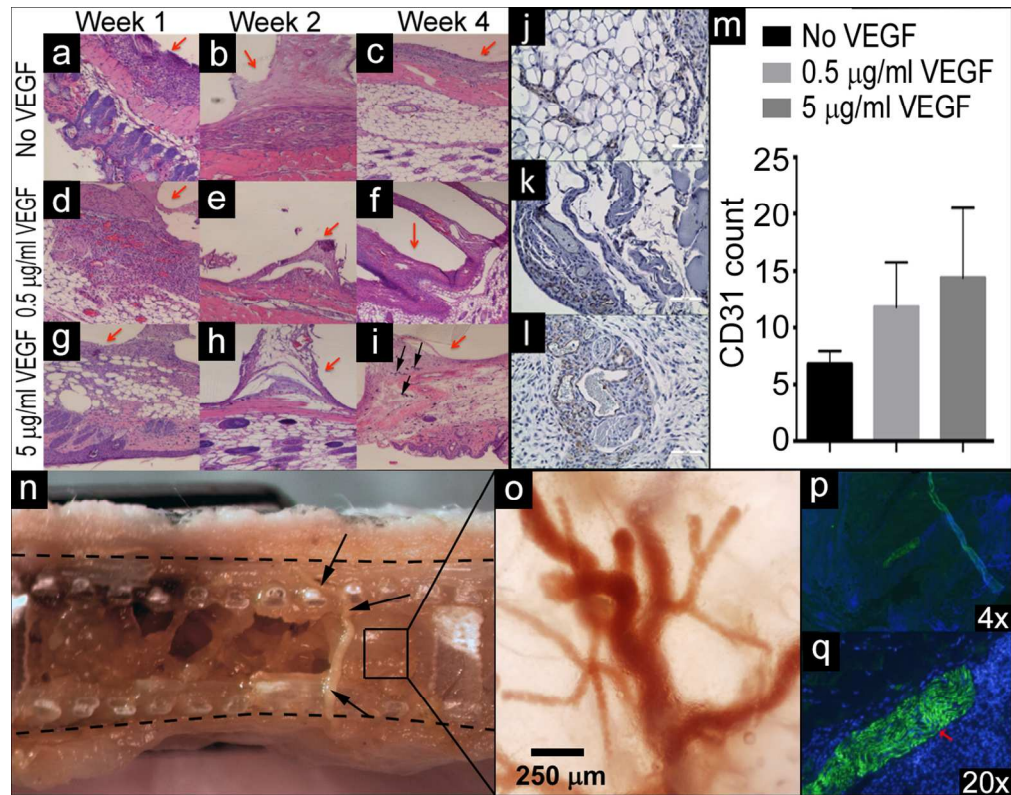
10  
11 **Figure 2.** H&E of the tissue surrounding the device at 4x. Tissue response at the device-subcutaneous  
12 tissue interface is shown (red arrow, a-i). Different concentrations of VEGF were tested and device  
13 retrieved after 1, 2, and 4 weeks from the implantation. CD31 staining of tissue (j-l). Scale bar is 50  $\mu\text{m}$ .  
14 CD31 count for each group (m). Optical microscope visualization of the tissue collected from the  
15 device reservoir, showing the presence of mature vessels (n-o). Neurofilament staining (SMI312-R, in  
16 green) indicates the proximity of subcutaneous nerve bundles to the encapsulation system (p-q).

17  
18 **Figure 3.** Insulin release from kidney capsule (black) and encapsulation system (red) after glucose  
19 stimulation (a). On week 12 all the animal with insulin level below 0.125 uU/ml where treated by  
20 refilling the implant with additional 2000 IEQ (red arrow). Basal blood glucose levels (b) and body  
21 weight (c). Average and Standard Error of the Mean are represented. \*  $p < 0.05$ ; \*\*\*  $p < 0.001$ .



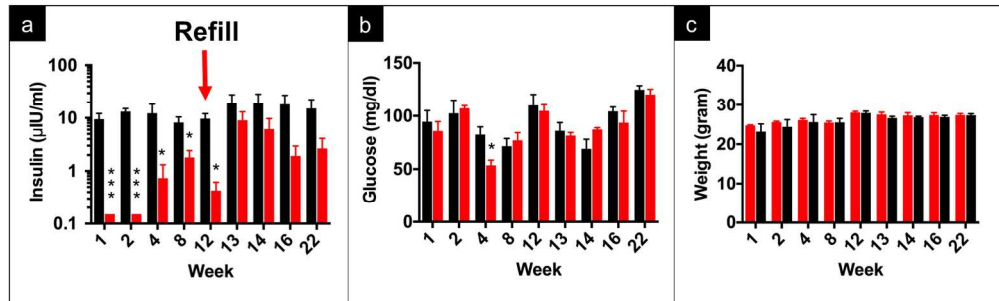
Mouse prototype of the 3D-printed PLA encapsulation device (a) and rendering of the structure (b) that includes insulin reservoirs (IR) and microchannels ( $\mu$ CH). Magnification of the microchannels under SEM (c and d). PLA superficial roughness measurements after Argon and Oxygen plasma treatments, changing time of application (0, 30, 90, 120, and 150 seconds) (e). AFM pictures of PLA surface treated with Oxygen plasma after 0, 90 and 120 seconds (f). Average and SEM are represented. \*\*  $p < 0.01$ .

719x666mm (72 x 72 DPI)



H&E of the tissue surrounding the device at 4x. Tissue response at the device-subcutaneous tissue interface is shown (red arrow, a-i). Different concentrations of VEGF were tested and device retrieved after 1, 2, and 4 weeks from the implantation. Diffuse spots of calcification (black arrows) were present at week 4 with the highest VEGF concentration (i). CD31 staining of tissue (j-l). Scale bar is 50 µm. Average and SEM of the CD31 count for high power field (m). Representative optical microscope visualization of the tissue collected from the device reservoir (VEGF 0.5 µg/ml group), showing the presence of mature vessels (n-o) Dotted lines represent device-subcutaneous tissue interface and the black arrows follow the path of a vessel through the polymeric scaffold. Neurofilament staining (SMI312-R, in green) indicates the proximity of subcutaneous nerve bundles to the encapsulation device (p-q).

499x393mm (72 x 72 DPI)



Insulin release from kidney capsule (black) and encapsulation device (red) after glucose stimulation (a). On week 12 all the animal with insulin level below  $0.125 \mu\text{U/ml}$  were treated by refilling the implant with additional  $2000 \text{ IEQ}$  (red arrow). Basal blood glucose levels (b) and body weight (c). Average and SEM are represented. \*  $p < 0.05$ ; \*\*\*  $p < 0.001$ .

318x95mm (150 x 150 DPI)

Peer Review

### 3D printed vascularized device for subcutaneous transplantation of human islets

**Authors:** Marco Farina<sup>\*1,4</sup>, Andrea Ballerini<sup>\*1,5</sup>, Daniel Fraga<sup>2</sup>, Eugenia Nicolov, Matthew Hogan<sup>3</sup>, Danilo Demarchi<sup>4</sup>, Francesco Scaglione<sup>5</sup>, Oaima Sabek<sup>2</sup>, Philip Horner<sup>3</sup>, Usha Thekkedath<sup>1</sup>, Osama Gaber<sup>\*\*2</sup>, Alessandro Grattoni<sup>\*\*1</sup>

<sup>1</sup>Department of Nanomedicine, Houston Methodist Research Institute, Houston, TX; <sup>2</sup>Department of Surgery, Houston Methodist Hospital, Houston, TX; <sup>3</sup>Center for Neuroregeneration, Houston Methodist Research Institute, Houston, TX; <sup>4</sup>Department of Electronics and Telecommunications, Politecnico di Torino, Torino, Italy; <sup>5</sup>Department of Oncology and Onco-Hematology, University of Milan, Milan, Italy

\*Co-first; \*\* Co-senior.

**Correspondence:** Dr. Alessandro Grattoni, Chair, Department of Nanomedicine, Houston Methodist Research Institute, 6670 Bertner Avenue, R8-216, Houston, TX, 77030

**E-mail:** agrattoni@houstonmethodist.org

**Keywords:** 3D printing, Diabetes, Encapsulation, Islets, Transplantation

**Abbreviations:** **FDM**, Fused Deposition Method; **H&E**, hematoxylin and eosin; **IEQ**, Islet equivalent; **PLM**, platelet lysate matrix; **PLA**, polylactic acid; **SEM**, scanning electron microscopy; **VEGF**, vascular endothelial growth factor.

**Abstract**

Transplantation of pancreatic islets or stem cell derived insulin secreting cells is an attractive treatment strategy for diabetes. However, islet transplantation is associated with several challenges including function-loss associated with dispersion and limited vascularization as well as the need for continuous immunosuppression. To overcome these limitations, here we present a novel 3D printed and functionalized encapsulation device for subcutaneous engraftment of islets or islet like cells. The devices were 3D printed with polylactic acid and the surfaces treated and patterned to increase the hydrophilicity, cell attachment and proliferation. Surface treated encapsulation systems were implanted with growth factor enriched platelet gel, which helped to create a vascularized environment before loading human islets. The device protected the encapsulated islets from acute hypoxia and kept them functional. The adaptability of the encapsulation system was demonstrated by refilling some of the experimental groups transcutaneously with additional islets.

## Introduction

Transplantation of pancreatic islets or stem cell derived insulin secreting cells is an attractive treatment strategy for diabetes<sup>1,2</sup>. However, islet transplantation is associated with several challenges including function-loss associated with dispersion and limited vascularization as well as the continuous need for immunosuppression<sup>3</sup>. In spite of early success with intrahepatic transplantation, widespread use of islet transplantation has been hampered by poor long-term survival of the graft<sup>3,4</sup>. After intra-hepatic or intravascular islet transplantation, graft function is lost rapidly due to dispersion of transplanted tissue, damage to graft caused by blood-mediated inflammatory reaction, and the hypoxic stress due to the limited ingrowth of new blood vessels<sup>5</sup>. High oxygen demand and the need for physiological architecture necessitate a highly vascularized and three-dimensional system for the long-term survival and function of transplanted islets. In addition, a minimally invasive and accessible site is fundamental for implantation, replenishment and graft retrieval. Retrieval is important when using engineered stem cells, whose long term fate and potential for tumor formation are not well known.<sup>6</sup> The subcutaneous space could serve as an ideal implantation site, if we can overcome challenges of low oxygen tension and poor vascularity and offer mechanical protection to transplanted cells<sup>7,8</sup>. To meet these needs, we designed an adaptable, scalable and refillable encapsulation system for subcutaneous transplantation of cells. In this work, we demonstrate the feasibility to 3D print an innovative encapsulation system and evaluate its vascularization after subcutaneous implantation. The system was loaded transcutaneously with human pancreatic islets and their long-term survival and function were studied in an immunocompromised mouse model.

## Materials & Methods

Discoidal encapsulation devices (8 mm in diameter and 2.5 mm in thickness, Fig. 1a) suitable for **rodent studies to hold** up to 5,000 islets were printed adopting a Fused Deposition Method (FDM) based 3D printer (Replicator™ 2X, MakerBot Industries) and medical grade polylactic acid (PLA, Foster Corporation). The two inner surfaces were composed of an array of **islet reservoirs** (300 μm x 300 μm) to house the transplanted islets individually, maintaining them in close proximity while avoiding clustering. These **islet reservoirs** are connected to surrounding tissues by an array of square

1  
2  
3 microchannels (100  $\mu\text{m}$  x 100  $\mu\text{m}$  cross section, 50  $\mu\text{m}$  length) to allow for the growth of  
4  
5 transmembrane blood vessels in view of graft vascularization. A rendering of this microstructure was  
6  
7 designed with a 3D CAD software (SolidWorks®) and is represented in Figure 1b. The devices  
8  
9 featured a loading port (1 mm diameter) for transcutaneous cell loading. Device surfaces were treated  
10  
11 with Argon and Oxygen plasma (March plasma etcher, Nordson). The power (30W) and gas flow  
12  
13 (150mTorr) were kept constant, while changing the exposure time (30, 90, 120 and 150 seconds). The  
14  
15 structure of the device was evaluated at different magnification by scanning electron microscopy  
16  
17 (SEM) (Nova NanoSEM, FEI) for channel quality and size (Fig. 1c-d). Hydrophilicity was evaluated by  
18  
19 measuring the water contact angle, as described previously<sup>9</sup> and surface nanopatterning and roughness  
20  
21 were evaluated by atomic-force microscopy set in tapping mode (Fig. 1e-f, BioScope Catalyst, Bruker  
22  
23 Instruments, Texas).

24  
25 The encapsulation devices were evaluated in nude mice (Nu/Nu, female, 8-10 week old), after  
26  
27 receiving approval by the Institutional Animal Care and Use Committee of Houston Methodist  
28  
29 Research Institute. The devices were sterilized with 70% ethanol and UV before performing all the  
30  
31 surface modification treatment with oxygen or argon plasma in a sterile environment (clean room of  
32  
33 the Houston Methodist Research Institute). Thereafter, devices were filled with a platelet-lysate  
34  
35 solution (ZenBio), under aseptic conditions and incubated overnight at 37 °C in a cell incubator to  
36  
37 form the gel, with the addition of bovine thrombin (BioPharm Laboratories, LLC). The ready to be  
38  
39 implanted devices were then packaged and transferred to the animal facility and the package opened  
40  
41 in a sterile environment just before the implantation. Surface treated and sterilized devices, loaded  
42  
43 with platelet-lysate matrix (PLM) enriched with VEGF at two different concentrations (0.5 and 5  
44  
45  $\mu\text{g}/\text{ml}$ ), were implanted subcutaneously in the mice dorsum (n=12 per group). At 1, 2, and 4 weeks  
46  
47 post implantation, 4 mice per group were euthanized and the graft explanted for histological  
48  
49 assessment of vascularization and innervation. The implant and surrounding tissues were harvested,  
50  
51 and processed for histopathology evaluation of tissue response to the implanted device with  
52  
53 hematoxylin and eosin (H&E). This staining was used to analyse tissue morphology and to evaluate  
54  
55 the presence of immune cells, vessels infiltration, and fibrotic response at the tissue-device interface.  
56  
57 CD31 antibody (Abcam, ab28364) was used for immunohistochemistry (IHC) analysis and a pan-  
58  
59  
60

1  
2  
3 axonal antibody (Cambridge Bioscience, SMI-312R-100) with immunofluorescence (IF) to assess  
4 device vascularization and innervation respectively. CD31 expressing cells were counted separately in  
5 10 high-power fields. (HPFs).  
6  
7

8  
9 A second experiment was performed in nude mice (n=5 per group) to evaluate insulin release from  
10 human islets transplanted into a prevascularized device. Human pancreatic islets (2,000 IEQ per mice)  
11 were injected subcutaneously with a 22 G needle into the encapsulation system 4 weeks after device  
12 implantation or were inserted under the kidney capsule (positive control).<sup>10</sup> Human insulin (ultra-  
13 sensitive human insulin ELISA kit, Alpco) and blood glucose (OneTouch® Glucometer, Johnson and  
14 Johnson) levels were assessed weekly and body weight was monitored throughout the experiment.  
15  
16 Intra peritoneal glucose tolerance test (IPGTT) was performed weekly to stimulate insulin secretion  
17 from the transplanted islets. Blood was collected using retro-orbital method, under topical anaesthesia  
18 and aseptic techniques. A subsequent test was performed on the same animal cohort to demonstrate  
19 the subcutaneous refillability of the implant. Twelve weeks after the first injection, additional human  
20 islets (2,000 IEQ per mice) were injected transcutaneously in all groups where the insulin production  
21 was lower than 0.125  $\mu$ IU/ml.  
22  
23

24  
25 Statistical analysis was performed using Student's two tailed paired t-test. Results are presented as  
26 mean and standard error of the mean (SEM). A value of  $p < 0.05$  was considered statistically significant.  
27  
28 GraphPad Software, Inc. was used for the analysis.  
29  
30  
31  
32  
33

## 34 **Results & Discussion**

35  
36 Transplantation of cells on porous biomaterials has emerged as a promising strategy for long-term  
37 function facilitating rapid tissue ingrowth, vascularization and innervation providing oxygen,  
38 nutrition, and waste removal<sup>11</sup>. Recognizing such needs for an islet and cell encapsulation system, we  
39 are working on new strategies to deliver cells subcutaneously<sup>9,12</sup>. The architecture of the proposed  
40 device is designed to maintain pancreatic islets close to blood vessels, but separated from each other  
41 to mimic the physiological architecture in the pancreas and avoid cell crowding.  
42  
43

44  
45 To increase the biointegration of the encapsulation system, we decided to use PLA, which is a  
46 widely adopted polymer in biomedical devices, biocompatible, and presents good elasticity and  
47  
48  
49  
50  
51  
52  
53  
54  
55  
56  
57  
58  
59  
60

1  
2  
3 mechanical strength suitable for subcutaneous implantation<sup>13-15</sup>. Due to the chiral nature of lactic acid,  
4  
5 PLA is hydrophobic with low cell adhesion properties. Surface treatment with plasma improves the  
6  
7 low surface free energy of different materials and offers a solvent-free technique capable of changing  
8  
9 the wettability, surface roughness and surface chemistry of polymers, enhancing cell proliferation and  
10  
11 viability<sup>16-18</sup>. Plasma activation also increases PLA's surface free energy forming a broad variety of  
12  
13 functional groups on the surface, including polar groups, which drastically change wettability and have  
14  
15 a positive effect on material-cell interactions. Previous work from our group demonstrated that  
16  
17 plasma treatment substantially increased the hydrophilicity of the surface and reduced the contact  
18  
19 angle, which remained stable over 30 days in phosphate buffered saline (PBS)<sup>9</sup>. Here we looked at the  
20  
21 effect of plasma exposure time on surface patterning and roughness and compared Oxygen and Argon  
22  
23 treatments. **Since UV light sterilization methods showed to increase polymer wettability without**  
24  
25 **affecting morphology and mechanical properties, we decide to evaluate the effect of the surface**  
26  
27 **modification only at the end of plasma treatment<sup>19</sup>**. As shown in Fig. 1e, both treatments increased  
28  
29 surface roughness, reaching a maximum value, after which the roughness diminished with continued  
30  
31 exposure, possibly due to eventual etching of the crystalline regions. It was also noticed that the  
32  
33 Oxygen treatment cause deeper patterns (4.63 nm with Argon and 26.45 nm with Oxygen,  $p < 0.01$ , Fig.  
34  
35 1f), which has been demonstrated to be beneficial for cell attachment and proliferation. **For this**  
36  
37 **reason, a 120 seconds Oxygen treatment was selected for the following experiments.**

40 We then investigated the in vivo vascularization and innervation of Oxygen treated devices  
41  
42 after subcutaneous implantation in nude mice. Nude mice were selected for these studies with the  
43  
44 novel encapsulation device as they show an inflammatory response to a foreign body, but allow for  
45  
46 transplantation with human islets without the need for immunosuppression. It has been broadly  
47  
48 demonstrated that vascularization of the graft is the key for successful engraftment of islet  
49  
50 transplants<sup>7,20</sup>. Prevascularization could mitigate the issue of acute hypoxia which was shown to result  
51  
52 in islet apoptosis and graft failure<sup>3</sup>. To stimulate neovascularization and to support the islet viability  
53  
54 and function for a period of time after transplantation we tested devices loaded with biological gels  
55  
56 with different VEGF concentrations<sup>21-23</sup>. An acute inflammatory response to the foreign body was  
57  
58 present in the first week after device implantation, mainly in the VEGF groups, and subsided with time,  
59  
60

1  
2  
3 leaving a rim of vascularized connective tissue around the device at week 4 (Fig. 2). Indeed, the  
4  
5 neutrophils, which are considered to have an impact on the development of the inflammatory  
6  
7 response leading to the formation of the fibrotic capsule<sup>24</sup>, were almost absent from the second week  
8  
9 (Fig. 2 a-i). The red arrows in Fig. 2 indicate the protrusion of the surrounding subcutaneous tissue  
10  
11 into the devices. Tissue samples were taken from the side of the device closer to the skin, representing  
12  
13 the subcutaneous environment. We noticed a positive trend between VEGF concentration and the  
14  
15 number of vessels stained by CD31 (Fig. 2j-m), **but there was no statistically significant difference**  
16  
17 **between the groups after 1 week, probably for the limited number of animals per group.** After 4 weeks,  
18  
19 we noticed calcification in the VEGF 5 µg/ml sample as evident by the dark spots in high density close  
20  
21 to the tissue-implant interface (Fig. 2i, black arrow). **It has been already shown that VEGF is involved**  
22  
23 **in the calcification process of cartilage<sup>25</sup> and at similar concentration it was tested to induce bone**  
24  
25 **response to implanted craniofacial implants<sup>26</sup>.** It was observed that in 4 weeks the subcutaneous tissue  
26  
27 and the inside of the device were **also vascularized with lower concentration of VEGF (Fig. 2n-o).**  
28  
29 Based on these results, 0.5 µg/ml VEGF was selected for further studies.

30  
31  
32 **Finally, we also found nerve bundles in the proximity of the device (Fig. 2p-q). These may have**  
33  
34 **reached the device and the transplanted islets. However, further long term studies are necessary to**  
35  
36 **prove and quantify islet innervation, considering the slower rate of growth of nerves compared to**  
37  
38 **vessels.**

39  
40 After proving the device vascularization, we performed a second experiment injecting human islet into  
41  
42 a prevascularized device **previously loaded with the VEGF rich matrix. By the time of the islet injection**  
43  
44 **the gel was already degraded, releasing growth factors (Fig. 2n).** We observed detectable levels of  
45  
46 human insulin from week 4, but at lower levels compared to the positive control (p<0.001). As  
47  
48 described in various islet encapsulation models, there is a lag time for adequate function until the  
49  
50 transplanted islets are vascularized<sup>7,27</sup>. The prevascularization of the device appeared to have helped  
51  
52 encapsulated islets to overcome the initial post implant injury, but it takes longer for the transplanted  
53  
54 cells to develop mature vasculature and be functional. **The lower insulin level detected after IPGTT in**  
55  
56 **the device group as compared to the kidney capsule control could be ascribed to a non-complete**  
57  
58 **vascularization of islets in the device. Although prevascularized, it is expected that islets will need to**  
59  
60

1  
2  
3 fully connect to the vasculature post transplantation. The duration of this process is compatible with  
4  
5 the 2 weeks timeframe observed in Fig.3 for an increase in insulin secretion in the device group. As the  
6  
7 platelet lysate matrix is expected to be resorbed within few days from device implantation, we do not  
8  
9 expect that islets were affected in their function by residual PLM. A second load of islets (2,000 IEQ)  
10  
11 into vascularized devices increased the insulin levels ( $\sim 10 \mu\text{IU/ml}$ ) to values that were comparable to  
12  
13 the kidney capsule transplantation (Fig. 3a,  $p > 0.05$ ). The total number of islets loaded was 4,000 IEQ  
14  
15 per device, less than the theoretical maximal loadable volume according to the three-dimensional  
16  
17 structure of device and the presence of a vascularized environment. Nevertheless, it was not possible  
18  
19 to estimate exact volume of vessels and tissue present in the device at the time of the second islet  
20  
21 loading, and this could have an effect on the distribution and the packing density of the islets in the  
22  
23 device. Further studies are required to understand the optimal timing and the amount of islets needed  
24  
25 to obtain a valid insulin secretion after multiple loading of islets. Achieving this could help adapting  
26  
27 the insulin output to patient physiology and clinical need. Additionally, the devices were well tolerated  
28  
29 and animals showed comparable basal glucose level (Fig. 3b) and weight (Fig. 3c), demonstrating that  
30  
31 the presence of additional islets is not associated with hypoglycemia.  
32  
33

### 34 35 36 **Conclusion**

37  
38 In this study, we showed that the subcutaneous implantation of a 3D printed and functionalized cell  
39  
40 encapsulation device generates adequate and prompt vascularization of the graft. Vascularization was  
41  
42 enhanced by the ability to dispense pro-angiogenic factors, such as VEGF, which is also known to  
43  
44 increase islet viability and function<sup>22</sup>. In addition, the device could protect the graft, while the islets are  
45  
46 being vascularized, from initial transplant site stressors and support their long-term survival. The  
47  
48 transcuteaneous refillability of the device offers opportunities for cell supplementation, without  
49  
50 surgical retrieval and re-implantation, to accommodate for changing physiological needs. This will be  
51  
52 of significant advantage in the case of the growing children with diabetes. Moreover, the reservoir  
53  
54 structure permits the potential retrievability of the graft, which is important for stem cell derived  
55  
56 engineered cells, undergoing malignant or other unwanted transformations. A current limitation of  
57  
58 this device is the lack of immunoprotection of the transplanted cells. The priority of this work was to  
59  
60

1  
2  
3 prove the vascularization and function of the device without compounding with the risk of immune  
4 rejection. For this reason, we used an immunodeficient animal model. A different device design can  
5 incorporate a strategy for local delivery of immunomodulators, which will expand its use in  
6 immunocompetent diabetic animals<sup>28,29</sup>. Further studies in diabetic animal models are required to  
7 evaluate the full potential of this versatile encapsulation device for diabetes cell therapy.  
8  
9  
10  
11  
12

### 13 14 15 **Acknowledgements**

16  
17 The authors express their sincere gratitude to the Vivian L. Smith Foundation for the funding support,  
18 and The Methodist Physician organization that made this investigation possible. Pancreata was  
19 provided by LifeGift Organ Procurement Organization, Houston Texas. Some research islets were  
20 provided by the Integrated Islet Distribution Program (City of Hope, Duarte CA). We thank Dr. Jianhua  
21 (James) Gu from the electron microscopy core, Dr. Andreana L. Rivera and Dr. Yulan Ren from the  
22 research pathology core of the Houston Methodist Research Institute.  
23  
24  
25  
26  
27  
28  
29  
30  
31

### 32 **Conflict of interest**

33  
34 Authors declare that they have competing interests as the encapsulation system described in this  
35 paper is currently under invention disclosure.  
36  
37  
38  
39  
40  
41  
42  
43  
44  
45  
46  
47  
48  
49  
50  
51  
52  
53  
54  
55  
56  
57  
58  
59  
60

## References

1. Ahearn, A. J., Parekh, J. R. & Posselt, A. M. Islet transplantation for Type 1 diabetes: where are we now? *Expert Rev. Clin. Immunol.* **11**, 59–68 (2015).
2. Zinger, A. & Leibowitz, G. Islet transplantation in type 1 diabetes: hype, hope and reality - a clinician's perspective. *Diabetes Metab. Res. Rev.* **30**, 83–87 (2014).
3. Brennan, D. C. *et al.* Long-Term Follow-Up of the Edmonton Protocol of Islet Transplantation in the United States. *Am. J. Transplant. Off. J. Am. Soc. Transplant. Am. Soc. Transpl. Surg.* (2015). doi:10.1111/ajt.13458
4. Shapiro, A. M. J. *et al.* International trial of the Edmonton protocol for islet transplantation. *N. Engl. J. Med.* **355**, 1318–30 (2006).
5. Lau, J. *et al.* Beneficial role of pancreatic microenvironment for angiogenesis in transplanted pancreatic islets. *Cell Transplant.* **18**, 23–30 (2009).
6. Pagliuca, F. W. & Melton, D. A. How to make a functional beta-cell. *Development* **140**, 2472–2483 (2013).
7. Pepper, A. R. *et al.* A prevascularized subcutaneous device-less site for islet and cellular transplantation. *Nat. Biotechnol.* **33**, 518–23 (2015).
8. Andrades, P. *et al.* Subcutaneous pancreatic islet transplantation using fibrin glue as a carrier. *Transplant. Proc.* **39**, 191–2 (2007).
9. Sabek, O. M. *et al.* Three-dimensional printed polymeric system to encapsulate human mesenchymal stem cells differentiated into islet-like insulin-producing aggregates for diabetes treatment. *J. Tissue Eng.* **7**, 2041731416638198 (2016).
10. Sabek, O. M., Fraga, D. W., Minoru, O., McClaren, J. L. & Gaber, A. O. Assessment of human islet viability using various mouse models. *Transplant. Proc.* **37**, 3415–6 (2005).
11. Scharp, D. W. & Marchetti, P. Encapsulated islets for diabetes therapy: History, current progress, and critical issues requiring solution. *Adv. Drug Deliv. Rev.* **67–68**, 35–73 (2014).
12. Sabek, O. M. *et al.* Characterization of a nanogland for the autotransplantation of human pancreatic islets. *Lab. Chip* **13**, 3675–88 (2013).

- 1  
2  
3 13. Onuki, Y., Bhardwaj, U., Papadimitrakopoulos, F. & Burgess, D. J. A review of the  
4 biocompatibility of implantable devices: current challenges to overcome foreign body response. *J.*  
5 *Diabetes Sci. Technol.* **2**, 1003–15 (2008).  
6  
7
- 8  
9 14. Lasprilla, A. J. R., Martinez, G. A. R., Lunelli, B. H., Jardini, A. L. & Filho, R. M. Poly-lactic acid  
10 synthesis for application in biomedical devices - a review. *Biotechnol. Adv.* **30**, 321–8 (2012).  
11  
12
- 13 15. *Poly(Lactic Acid): Synthesis, Structures, Properties, Processing, and Applications.* (John Wiley &  
14 Sons, Inc., 2010).  
15  
16
- 17 16. Shah, A., Shah, S., Mani, G., Wenke, J. & Agrawal, M. Endothelial cell behaviour on gas-plasma-  
18 treated PLA surfaces: the roles of surface chemistry and roughness. *J. Tissue Eng. Regen. Med.* **5**,  
19 301–12 (2011).  
20  
21  
22
- 23 17. Jacobs, T. *et al.* Plasma surface modification of polylactic acid to promote interaction with  
24 fibroblasts. *J. Mater. Sci. Mater. Med.* **24**, 469–478 (2012).  
25  
26
- 27 18. Morent, R., De Geyter, N., Desmet, T., Dubruel, P. & Leys, C. Plasma Surface Modification of  
28 Biodegradable Polymers: A Review. *Plasma Process. Polym.* **8**, 171–190 (2011).  
29  
30
- 31 19. Valente, T. A. M. *et al.* Effect of Sterilization Methods on Electrospun Poly(lactic acid) (PLA)  
32 Fiber Alignment for Biomedical Applications. *ACS Appl. Mater. Interfaces* **8**, 3241–3249 (2016).  
33  
34
- 35 20. Pepper, A. R., Gala-Lopez, B., Ziff, O. & Shapiro, A. M. J. Revascularization of transplanted  
36 pancreatic islets and role of the transplantation site. *Clin. Dev. Immunol.* **2013**, 352315 (2013).  
37  
38  
39
- 40 21. Jabs, N. *et al.* Reduced insulin secretion and content in VEGF-a deficient mouse pancreatic  
41 islets. *Exp. Clin. Endocrinol. Diabetes Off. J. Ger. Soc. Endocrinol. Ger. Diabetes Assoc.* **116 Suppl**, S46–  
42 9 (2008).  
43  
44  
45
- 46 22. Lammert, E. *et al.* Role of VEGF-A in vascularization of pancreatic islets. *Curr. Biol. CB* **13**,  
47 1070–4 (2003).  
48  
49
- 50 23. Watada, H. Role of VEGF-A in pancreatic beta cells. *Endocr. J.* **57**, 185–191 (2010).  
51  
52
- 53 24. Anderson, J. M., Rodriguez, A. & Chang, D. T. Foreign body reaction to biomaterials. *Semin.*  
54 *Immunol.* **20**, 86–100 (2008).  
55  
56  
57  
58  
59  
60

- 1  
2  
3 25. Patil, A. S., Sable, R. B. & Kothari, R. M. Occurrence, biochemical profile of vascular endothelial  
4 growth factor (VEGF) isoforms and their functions in endochondral ossification. *J. Cell. Physiol.* **227**,  
5 1298–1308 (2012).  
6  
7  
8  
9 26. Ramazanoglu, M. *et al.* Bone response to biomimetic implants delivering BMP-2 and VEGF: an  
10 immunohistochemical study. *J. Cranio-Maxillo-fac. Surg. Off. Publ. Eur. Assoc. Cranio-Maxillo-fac.*  
11 *Surg.* **41**, 826–835 (2013).  
12  
13  
14  
15 27. Szot, G. L. *et al.* Tolerance induction and reversal of diabetes in mice transplanted with human  
16 embryonic stem cell-derived pancreatic endoderm. *Cell Stem Cell* **16**, 148–157 (2015).  
17  
18  
19 28. Ferrati, S. *et al.* Leveraging nanochannels for universal, zero-order drug delivery in vivo. *J.*  
20 *Control. Release Off. J. Control. Release Soc.* **172**, 1011–9 (2013).  
21  
22  
23  
24 29. Van Belle, T. & von Herrath, M. Immunosuppression in islet transplantation. *J. Clin. Invest.* **118**,  
25 1625–1628 (2008).  
26  
27  
28  
29  
30  
31  
32  
33  
34  
35  
36  
37  
38  
39  
40  
41  
42  
43  
44  
45  
46  
47  
48  
49  
50  
51  
52  
53  
54  
55  
56  
57  
58  
59  
60

1  
2  
3 **Figure 1.** Mouse prototype of the 3D-printed PLA encapsulation device (a) and rendering of the  
4 structure (b) that includes insulin reservoirs (IR) and microchannels ( $\mu$ CH). Magnification of the  
5 microchannels under SEM (c and d). PLA superficial roughness measurements after Argon and Oxygen  
6 plasma treatments, changing time of application (0, 30, 90, 120, and 150 seconds) (e). AFM pictures of  
7 PLA surface treated with Oxygen plasma after 0, 90 and 120 seconds (f). Average and SEM are  
8 represented. \*\*  $p < 0.01$ .

9  
10  
11  
12  
13 **Figure 2.** H&E of the tissue surrounding the device at 4x. Tissue response at the device-subcutaneous  
14 tissue interface is shown (red arrow, a-i). Different concentrations of VEGF were tested and device  
15 retrieved after 1, 2, and 4 weeks from the implantation. Diffuse spots of calcification (black arrows)  
16 were present at week 4 with the highest VEGF concentration (i). CD31 staining of tissue (j-l). Scale bar  
17 is 50  $\mu$ m. Average and SEM of the CD31 count for high power field (m). Representative optical  
18 microscope visualization of the tissue collected from the device reservoir (VEGF 0.5  $\mu$ g/ml group),  
19 showing the presence of mature vessels (n-o) Dotted lines represent device-subcutaneous tissue  
20 interface and the black arrows follow the path of a vessel through the polymeric scaffold.  
21 Neurofilament staining (SMI312-R, in green) indicates the proximity of subcutaneous nerve bundles to  
22 the encapsulation device (p-q).

23  
24  
25  
26  
27  
28  
29  
30  
31 **Figure 3.** Insulin release from kidney capsule (black) and encapsulation device (red) after glucose  
32 stimulation (a). On week 12 all the animal with insulin level below 0.125 uU/ml were treated by  
33 refilling the implant with additional 2000 IEQ (red arrow). Basal blood glucose levels (b) and body  
34 weight (c). Average and SEM are represented. \*  $p < 0.05$ ; \*\*\*  $p < 0.001$ .